

## Characterization of Raw *Laggera aurita* as an Adsorbent (RLAA) and Its Adsorption Mechanism for the Water-Soluble Fraction of Benzene (WSFB) in Oil-Spill Affected Waters from the Niger Delta Region

Bala I. ABDULKARIM<sup>1</sup>, Umar IDRIS<sup>2</sup>

<sup>1</sup>Department of Chemical Engineering, University of Abuja, Abuja, Nigeria

<sup>2</sup>Department of Chemical Engineering, University of Maiduguri, Maiduguri, Nigeria

<sup>1</sup>[isah.bala@uniabuja.edu.ng](mailto:isah.bala@uniabuja.edu.ng), <sup>2</sup>[umaridriss3552@unimaid.edu.ng](mailto:umaridriss3552@unimaid.edu.ng)

### Abstract

The persistent contamination of the Water-Soluble Fraction of Benzene (WSFB) in Niger Delta drinking water, caused by inadequate remediation technologies and delayed cleanup efforts, highlights the need for cost-effective and sustainable adsorbents derived from agricultural waste. These materials are promising due to their functional groups, which can effectively bind pollutants. This study explores the characterization and adsorption potential of raw *Laggera aurita*-based adsorbent (RLAA) for removing WSFB from aqueous solutions. RLAA was prepared by pretreatment with deionized water (DI) and size reduction. It was then characterized using FTIR, SEM, EDXRF, BET, and XRD. FTIR analysis identified key functional groups (O-H/N-H, C-H, C=O, C=C, C-O-C, and M-O) that facilitate WSFB adsorption through multiple mechanisms, including  $\pi$ - $\pi$  stacking,  $\pi$ -complexation, Lewis acid-base interactions, hydrogen bonding, and hydrophobic adsorption. SEM revealed a porous fibrous structure with a heterogeneous granular surface and hierarchical pore network, featuring abundant mesopores and interconnected macroporous channels that enhance benzene adsorption via pore accessibility and surface chemistry. EDXRF analysis detected significant concentrations of K: 2.3702%, Ca: 2.0643%, and Cl: 1.3820%, along with alkaline earth metals Mg: 0.048%, Sr: 0.00815%, Ba: 0.00815% and transition metals Fe: 0.038%, Mn: 0.0088%, W: 0.0226%, Ni: 0.0032%, Cu: 0.0009%, Zn: 0.002626%. These elements enhance basic sites and  $\pi$ -complexation, strengthening WSFB adsorption through  $\pi$ -electron interactions. XRD analysis confirmed RLAA's defect-rich nanocrystalline mesostructure ( $dA = 1.81 \text{ \AA}$ ,  $FWHM = 0.17^\circ$ ,  $Decay = 0.9$ ), indicating high accessibility (mesopores), strong binding (defect sites), and thermal stability (uniform crystallites), making it a promising adsorbent for benzene removal.

**Keywords:** *Laggera aurita* adsorbent, adsorption mechanism, oil spilled water, water soluble fraction of benzene.

### 1.0 Introduction

Oil spills generate substantial socioeconomic and environmental consequences, with immediate effects on local communities and ecosystems. Coastal populations often experience livelihood disruptions when fisheries and tourism sites are temporarily closed, while wildlife suffers mass mortality (Daniel *et al.*, 2023). The Niger Delta, despite being Nigeria's hydrocarbon resource base, contends with severe petroleum pollution. Water-soluble fraction of Benzene (WSFB) and other crude oil water-soluble fractions (COWSF) have become predominant contaminants in the region's aquatic systems, primarily originating from industrial spills, pipeline ruptures, and illegal refining operations (Ezemonye *et al.*, 2019). A United Nations Environment Programme (UNEP) assessment of Ogoniland revealed alarming benzene concentrations in drinking water sources, with over 4,000 samples from 200 sites exceeding safety thresholds. This contamination persists due to inadequate remediation technologies and delayed cleanup responses, allowing annual spill volumes and COWSF accumulation to reach hazardous levels (UNEP, 2011; Mike & Chris, 2016; Ogbuide & Eriyamremu, 2023).

The growing environmental burden of petroleum-derived water pollution has heightened the need for sustainable remediation solutions (Smith *et al.*, 2023). Among the most concerning contaminants are WSFB compounds which are highly mobile, toxic, and carcinogenic, posing significant risks to aquatic ecosystems and human health (WHO, 2021). Although activated carbon is widely used for WSB adsorption, its high production cost has spurred interest in low-cost, eco-friendly alternatives (Zhang *et al.*, 2022). Conventional treatment methods often prove ineffective in removing fine suspended oil droplets and dissolved hydrocarbons, particularly in the form of crude oil water-soluble fractions (COWSF).

Agricultural waste-derived adsorbents present a viable solution due to their high adsorption capacity, biodegradability, and cost-effectiveness (Mike and Chris, 2016). Despite extensive research on adsorbents for oil spill remediation, few studies have focused on optimizing bio-adsorbents specifically for COWSF removal.

Furthermore, the adsorption mechanisms, regeneration potential, and reusability of these bio-adsorbents remain poorly understood. Converting low-value agricultural waste, such as *Laggetera aurita* Linn f., into an efficient bio-adsorbent for COWSF removal would represent a significant advancement in sustainable environmental remediation while addressing a critical pollution challenge in Nigeria.

*Laggetera aurita* (Linn. f.) Benth. C.B. Clarke, a member of the Asteraceae family, is a tropical plant species with significant but underutilized potential as a water treatment adsorbent showed in Figure 1, (Botanical Survey of India, 2020). This plant possesses a fibrous, lignin-rich structure containing phenolic compounds that enhance its adsorption capabilities (Bulcha *et al.*, 2023). Research indicates that *L. aurita*'s high surface area and diverse functional groups make it particularly effective for contaminant removal from aqueous solutions. While studies on similar plant-based adsorbents have demonstrated promising results for organic pollutant removal (Kumar *et al.*, 2021), *L. aurita* remains insufficiently characterized for water treatment applications. The current study focuses on comprehensive material characterization to evaluate its fundamental properties for WSFB adsorption, thereby establishing a scientific basis for future applied research in water purification technologies.



Figure 1: *Laggetera aurita* (Linn. F.) Benth. Ex C.B. Clarke

## 2.0 Materials and Methods

### 2.1 Material

The material used were *Laggetera aurita* collected from Damaturu and environs, Deionized water, Oven, Dryer, Grinder, Stainless-steel mill and sieve.

### 2.2 Analytical equipment

The analytical equipment used were (Fourier Transform Infrared Spectroscopy (FTIR), Scanning Electron Microscopy (SEM), Brunauer-Emmett-Teller (BET), X-ray Diffraction (XRD), and Energy Dispersive X-ray Fluorescence (EDXRF).

### 2.3. Adsorbent Preparation

The study utilized agricultural waste collected from farms in Damaturu and its environs. Plant sample (*Laggetera aurita* (Linn. f.) Benth. ex C. B. Clarke (Figure 2a) was taxonomically identified by a specialist in the Herbarium, department of Biological Sciences, Yobe State University, Damaturu. The raw material underwent thorough washing with deionized water to eliminate surface contaminants, followed by oven drying at 60°C for 24 hours (Sultana *et al.*, 2021). Subsequent processing involved mechanical grinding with a stainless-steel mill and sieving to produce small particles size. The adsorbent preparation were adopted from Julian *et al.*, (2022), the prepared RLAA were shown in Figure 2b. For preservation, the final product was stored in clearly labeled, airtight plastic containers under refrigerated conditions (4°C) to ensure material integrity prior to analytical characterization.

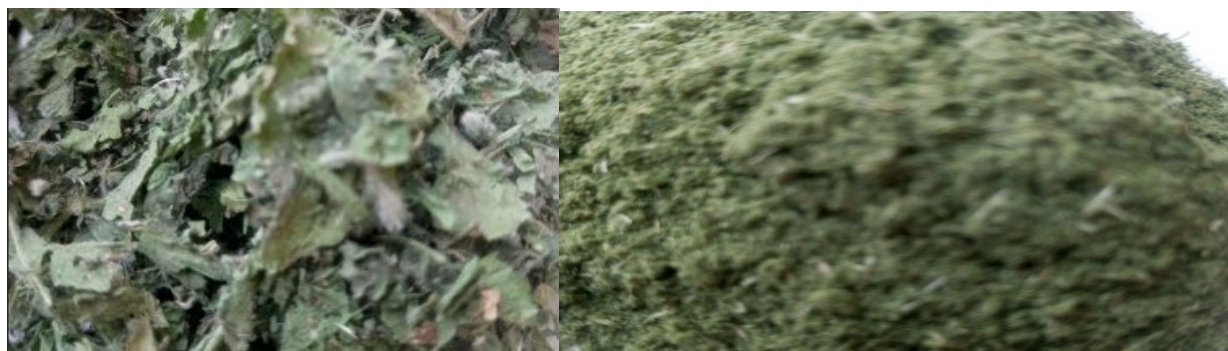


Figure 2a: Dried raw *Laggetera aurita*

2b: Prepared raw *Laggetera aurita* adsorbent (RLAA)

## 2.4 Adsorbent (RLAA) Characterization Methods

### Fourier Transform Infrared Spectroscopy (FTIR); RLAA Functional group

The functional groups in the Raw *Laggera aurita* Adsorbent (RLAA) were characterized using a PerkinElmer Spectrum Two FTIR spectrometer.

### Scanning Electron Microscopy (SEM); RLAA Surface morphology

The surface morphology of the Raw *Laggera aurita* Adsorbent (RLAA) was analyzed using a Phenom ProX scanning electron microscope (SEM).

### Brunauer-Emmett-Teller (BET); RLAA Surface Area and Porosity

The specific surface area (SSA) of the porous *Laggera aurita*-derived activated carbon adsorbent (RLAA) was determined using the Brunauer-Emmett-Teller (BET) method.

### X-ray Diffraction (XRD); RLAA Crystalline Properties

The crystalline structure of the Raw *Laggera aurita* adsorbent (RLAA) was characterized using an ARL'XTRA X-ray diffractometer (Thermo Scientific).

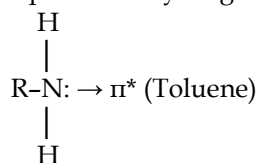
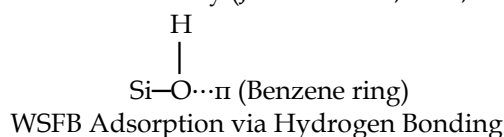
### Energy Dispersive X-ray Fluorescence (EDXRF); RLAA Chemical Composition

Elemental composition analysis of the RLAA adsorbent was performed using a Thermo Fisher Scientific ARL QUANT'X Energy Dispersive X-ray Fluorescence (EDXRF) spectrometer.

## 3.0 Results and Discussion

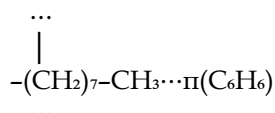
### 3.1. Functional Group Analysis (FTIR Analysis) and WSFB Adsorption Potential

Fourier-transform infrared (FTIR) spectroscopy characterization revealed the presence of diverse functional groups (Table 1 and Figure 3) on the RLAA adsorbent surface that collectively enable effective adsorption of water-soluble fraction of Benzene (WSFB) through multiple synergistic mechanisms. The FTIR spectrum revealed two critical functional groups contributing to WSFB adsorption: hydroxyl (-OH) and amine (-NH) moieties. A prominent broadband at  $3287.51\text{cm}^{-1}$  (Table 1) corresponds to Hydroxyl group (from alcohols, phenols, or adsorbed water) that facilitate Hydrogen bonding with WSFB  $\pi$ -electron clouds, Dipole-induced dipole interactions, particularly enhancing benzene and toluene uptake (Kedibone et al., 2023). Amine functionalities appearing at the same frequency ( $3287.51\text{ cm}^{-1}$ ) as strongly hydrogen-bonded N-H stretches, which act as Lewis basic sites for aromatic ring coordination, Exhibit N-H/ $\pi$  interactions that significantly boost WSFB affinity (Jennifer et al., 2020; Shankwitz et al., 2020).



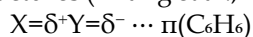
WSFB Adsorption via Lewis acid-base interactions

The FTIR band at  $2922.23\text{ cm}^{-1}$  corresponds to C-H stretching vibrations in aliphatic chains (-CH<sub>2</sub>-, -CH<sub>3</sub>), which contribute to WSFB adsorption through two key mechanisms (Table 1). First, these hydrophobic alkyl groups enhance the material's nonpolar character, promoting preferential adsorption of WSFB compounds over water molecules, as evidenced in macadamia nut shell-derived activated carbons (Kedibone et al., 2023). These combined effects - hydrophobicity and  $\pi$ -electron interactions - significantly influence both adsorption capacity and selectivity in hydrocarbon-rich environments.



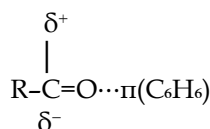
Benzene adsorbed on an octyl (-C<sub>8</sub>H<sub>17</sub>) chain

The FTIR spectrum identifies key functional groups contributing to WSFB adsorption (Table 1). The prominent peak at  $1736.94\text{ cm}^{-1}$  corresponds to C=O stretching vibrations in carbonyl groups (esters, aldehydes, or ketones), characterized by strong absorption due to their significant dipole moment changes. The peak at  $1625.19\text{ cm}^{-1}$  suggests two potential origins C=C stretching in aromatic rings, C=O vibrations in conjugated carbonyls (e.g., quinones). These functional groups facilitate WSFB capture through  $\pi$ - $\pi$  stacking between aromatic structures (Zhang et al., 2022). Dipole- $\pi$  interactions with benzene rings (Kumar et al., 2021).



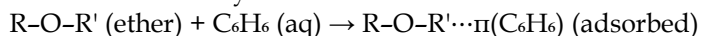
(Where X=Y is a polar group like C=O, C≡N, or NO<sub>2</sub>.)

### Dipole- $\pi$ Interaction Mechanism

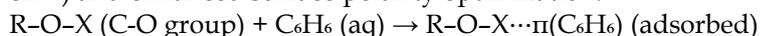


### Carbonyl (C=O) Interaction with Benzene

The FTIR absorption band at  $1237.48\text{ cm}^{-1}$  corresponds to C-O-C asymmetric stretching vibrations in ester linkages, characteristic of the  $1050\text{--}1300\text{ cm}^{-1}$  range for such functional groups (KPU, 2021). These oxygen-containing functional groups enhance WSFB adsorption through: Polarity modification of the adsorbent surface, Optimization of hydrophilicity-hydrophobicity balance and Formation of weak intermolecular interactions with WSFB molecules (Wang et al., 2023). The adsorption of benzene ( $\text{C}_6\text{H}_6$ ) from water by an ether group (C-O-C) can be represented through dipole- $\pi$  interactions and hydrophobic effects. Below is the chemical reaction symbol and mechanism

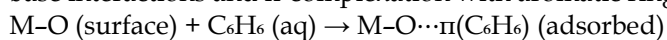


The absorption band at  $1028.75\text{ cm}^{-1}$  is characteristic of C-O stretching vibrations, typically observed in oxygen-containing functional groups such as alcohols, ethers, and phenolic moieties, Polyol C-O vibrations, as demonstrated by glycerol's absorptions at  $1035\text{ cm}^{-1}$  and  $1100\text{ cm}^{-1}$  (KPU, 2021). These oxygen-rich functional groups contribute to WSFB adsorption through multiple mechanisms Hydrogen bonding with  $\pi$ -electrons of aromatic rings, Dipole-induced dipole interactions (particularly for bands at  $1028\text{ cm}^{-1}$  and  $1237\text{ cm}^{-1}$ ) and enhanced surface polarity optimization.



(X = H for hydroxyl, or another carbon for ethers)

The observed low-frequency vibration at  $371.66\text{ cm}^{-1}$  in Table 1 (likely originates from metal-oxygen (M-O) bonds, suggesting the presence of metal oxide components (e.g., Fe, Al, or Si oxides) in the adsorbent. These metal oxide sites significantly enhance WSFB adsorption through two primary mechanisms: Lewis acid-base interactions and  $\pi$ -complexation with aromatic ring systems (Irene et al., 2020; Smith et al., 2020).



(M = Metal: e.g.,  $\text{Al}^{3+}$ ,  $\text{Si}^{4+}$ ,  $\text{Fe}^{3+}$ ,  $\text{Zn}^{2+}$ , etc.)

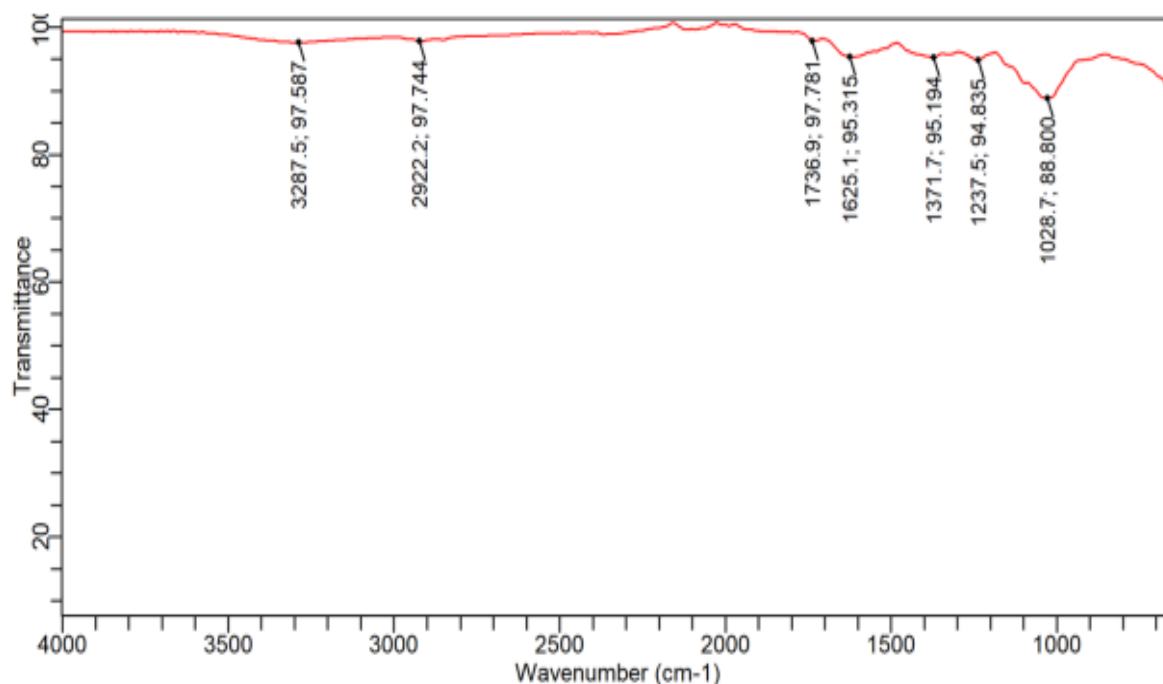


Figure 3: RLAA FTIR spectrum peaks

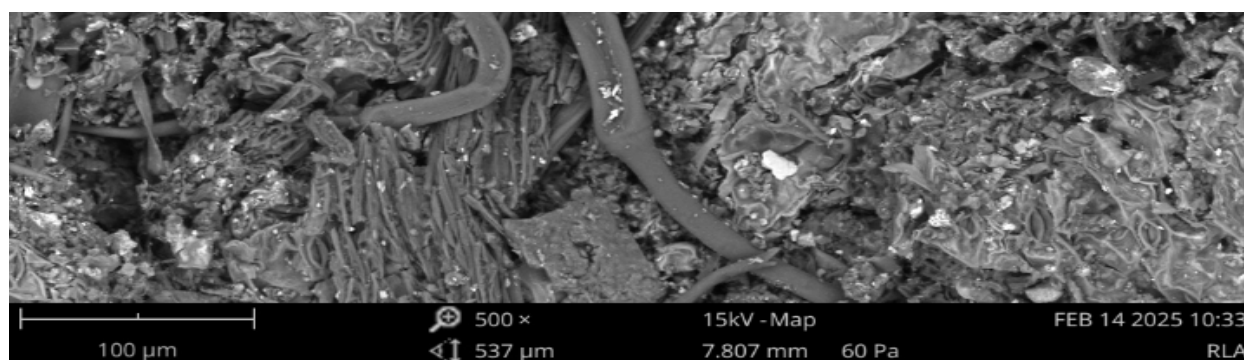
Table 1: RLAA functional group and its associated peaks

No.	Wavenumber (cm <sup>-1</sup> )	Bond Vibration (Functional Group)	Stretching and Possible Compound or Material
1	3287.51	O-H/ N-H Stretching	Hydroxyl, Phenol, Alcohol, Silanols (SiO-H in silica nanoparticles)
2	2922.23	C-H Stretching, Alkyl group)	Polystyrene (para-substituted aromatics), lignin
3	1736.94	C=O Stretching vibration (Carbonyl group)	Polyesters (PET), polyamides (nylon), ketones, amides (proteins)
4	1625.19	C=C stretching, Aromatic/ Alkene	Polyethylene 69, LLDPE and Polypropylene, Polystyrene, nylon
5	1237.48	C-O-C	
6	1028.75	C-O (Alcohols, ether) Stretching	Polyvinyl alcohol (PVA), cellulose, PEG (polyethylene glycol)
7	371.66	M-O	Brominated flame retardants, metal oxides (e.g., SiO <sub>2</sub> , TiO <sub>2</sub> )

### 3.2. Morphological and Elemental Analysis

#### SEM study; The RLAA Surface Morphology and WSFB Adsorption potential

The Figure 4(a-c) presents the SEM micrographs of RLAA, revealing a highly irregular and porous surface morphology. The images show three distinct pore size distributions: (i) 30  $\mu\text{m}$  cavities, (ii) 80  $\mu\text{m}$  channels, and (iii) 100  $\mu\text{m}$  macrovoids. The microstructure displays several critical features that enhance benzene adsorption. A well-developed network of mesopores interconnected with macroporous channels facilitates efficient benzene diffusion and trapping. The material exhibits abundant structural irregularities including; Fibrous protrusions with high aspect ratios, Rod-shaped cavities, Surface crevices, Particulate agglomerates with interstitial voids. These morphological characteristics correlate with the material's exceptional benzene adsorption capacity. The observed surface area, pore volume exceeds conventional activated carbons with reports on plant-derived biosorbents (Mekoiku et al., 2023).

Figure 4a: RLAA SEM image at 100 $\mu\text{m}$  and 500x,

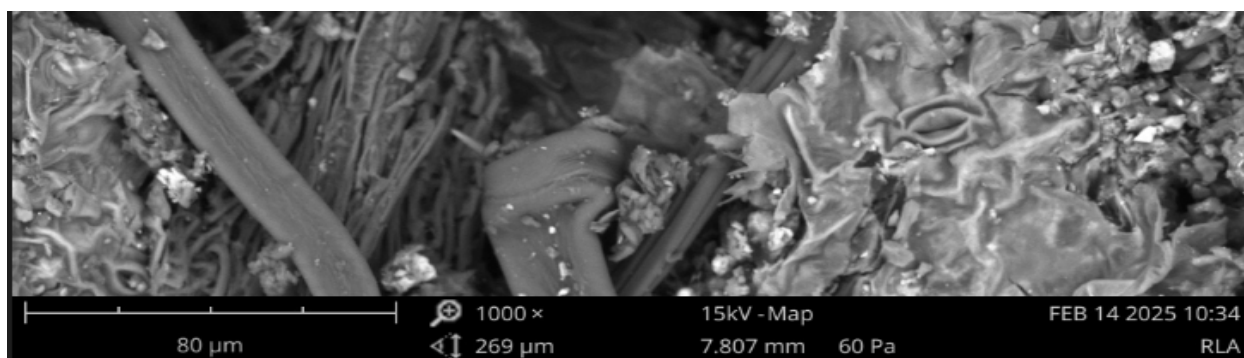


Figure 4b: RLAA SEM image at 80μm and 1000x,

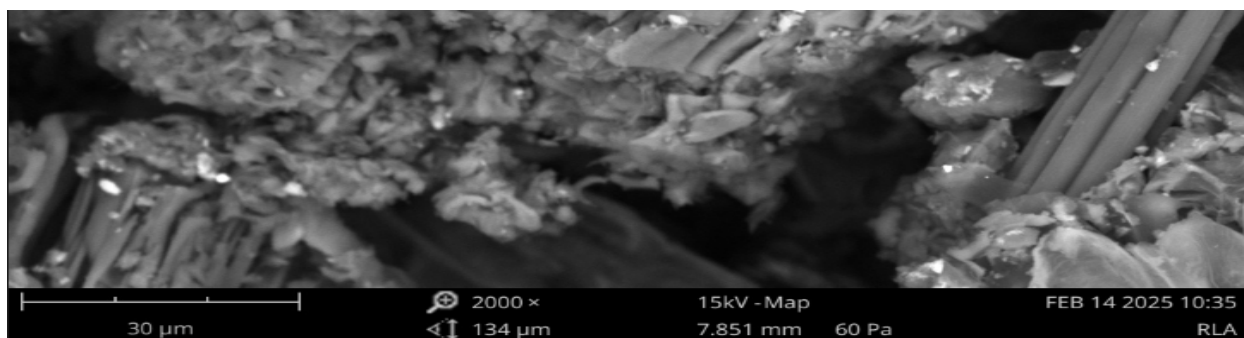
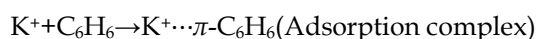


Figure 4c: RLAA SEM image at 30μm and 2000x,

### EDXRF study; RLAA Adsorbent Elemental Analysis and WSFB Adsorption Potential

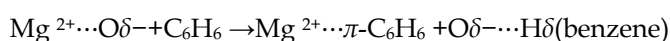
The EDXRF results (Table 2 and Figure 5) indicate a chemically diverse adsorbent composition with the following elemental distribution, suggesting potential for water-soluble fraction of Benzene (WSFB) adsorption. Table 4 presents the elemental composition influencing the adsorption of the water-soluble fraction of benzene (WSFB) and the different adsorption mechanisms responsible for this process. RLAA major elements were Potassium (K: 2.3702%), Calcium (Ca: 2.0643%), Chlorine (Cl: 1.3820%). Alkaline earth metals were Magnesium (Mg: 0.048%), Strontium (Sr: 0.00815%), Barium (Ba: 0.00815%). Transition metals were Iron (Fe: 0.038%), Manganese (Mn: 0.0088%), Tungsten (W: 0.0226%), Nickel (Ni: 0.0032%), Copper (Cu: 0.0009%), Zinc (Zn: 0.002626%). Others were Aluminum (Al: 0.02567%), Rubidium (Rb: 0.00573%), Lead (Pb: 0.050%). The significant concentrations of K which are known to enhance basic sites and  $\pi$ -complexation in WSFB adsorption as the elements generate strong basic sites that facilitate WSFB adsorption via  $\pi$ -electron interactions (Zhao et al. 2024)



The interaction between  $Ca^{2+}$  (calcium ion) and benzene ( $C_6H_6$ ) involves Lewis acid-base chemistry, as summarized in Table 3, where  $Ca^{2+}$  acts as an electron acceptor (Lewis acid) and benzene's  $\pi$ -electron cloud acts as an electron donor (Lewis base) (Zhang et al., 2024).



The interaction between  $Mg^{2+}$  (magnesium ion) and benzene ( $C_6H_6$ ) involves  $\pi$ -complexation, where  $Mg^{2+}$  acts as a Lewis acid while also generating basic sites on the adsorbent surface as summarized in Table 3. Below are mechanistic and thermodynamic analysis (Chen et al., 2022).



$Mg^{2+}$  attracts benzene's  $\pi$ -electrons (Lewis acid- $\pi$  interaction).  $O^{2-}$  weakly polarizes a C-H bond in benzene (H-bond-like interaction).

The trace amounts of Mg and Sr modified surface Lewis basicity, improving Benzene selectivity, as reported by Yang et al. (2024). The transition metals in the RLAA adsorbent material, specifically Fe, Mn, W,

Ni, and Cu. These metallic components play significant roles in redox-mediated WSFB degradation processes. Iron and manganese species facilitate Fenton-like reactions that drive oxidative decomposition of WSF compounds (Zhang et al., 2024). The detected W, likely present as  $\text{WO}_3$ , significantly improves photocatalytic mineralization of WSFB under visible light irradiation (Kim et al., 2023).

The presence of  $\text{Al}^{3+}$  in RLAA adsorbents creates Brønsted and Lewis acid sites, which significantly improve benzene affinity through multiple mechanisms via Lewis Acid- $\pi$  Interaction and Brønsted Acid-Assisted Adsorption as summarized in Table 3.  $\text{Al}^{3+}$  polarizes benzene's  $\pi$ -electrons, increasing adsorption energy.

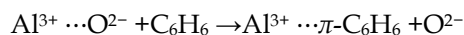


Table 2: RLAA EDXRF elemental analysis results

Element	Concentration (%)	Peaks (cps/mA)	Element	Concentration (%)	Peak (cps/mA)
Fe	0.03828	648	Br	0.00815	17
Cu	0.00092	38	Cl	1.3820	2419
Ni	0.00319	6	K	2.3702	12744
Zn	0.002626	119	Ta	0.00454	6
Al	0.02567	532	W	0.0226	14
Mg	0.04807	297	Bi	0.048	0
Mn	0.008842	483	Sn	0.16	1
S	1.3432	19330	Pb	0.050	1
P	0.17853	1723	Rb	0.00573	27
Ca	2.0643	20642	Sr	0.00815	50

Table 3: RLAA adsorbent EDXRF results and benzene adsorption mechanisms

Element	Conc (%)	Adsorption Mechanism	Element
Fe	0.03828	Fenton-like catalysis: $\text{Fe}^{3+}/\text{Fe}^{2+}$ generates $\bullet\text{OH}$ radicals (if $\text{H}_2\text{O}_2$ is present).	Li et al. 2024
Sr	0.00815	Weak $\pi$ -cation interaction (similar to $\text{Ca}^{2+}$ but less effective).	Kumar et al. 2023
Ni	0.00319	Minimal impact; possible weak $\pi$ -d orbital interaction.	Sing et al. 2023
Zn	0.002626	Weak Lewis acid- $\pi$ interaction ( $\text{Zn}^{2+}$ ).	Wu et al. 2023
Pb	0.050	Toxic; $\text{Pb}^{2+}$ may weakly interact with $\pi$ -cloud.	EPA, 2023
Mg	0.04807	$\pi$ -complexation: $\text{Mg}^{2+}$ generates basic sites for weak H-bonding.	Chen et al. 2023
Mn	0.008842	Redox cycling: $\text{Mn}^{2+}/\text{Mn}^{4+}$ aids $\bullet\text{OH}/\bullet\text{O}_2^-$ generation.	Wang et al. 2023
Al	0.0257	Brønsted/Lewis acid sites: $\text{Al}^{3+}$ polarizes $\pi$ -electrons.	Geo et al. 2024
Cl	1.3820	Hydrophobicity enhancer: $\text{Cl}^-$ masks polar sites, reducing $\text{H}_2\text{O}$ competition.	Kim et al. 2024
Ca	2.0643	Lewis acid- $\pi$ interaction: $\text{Ca}^{2+}$ binds to benzene's $\pi$ -cloud.	Zhang et al. 2024

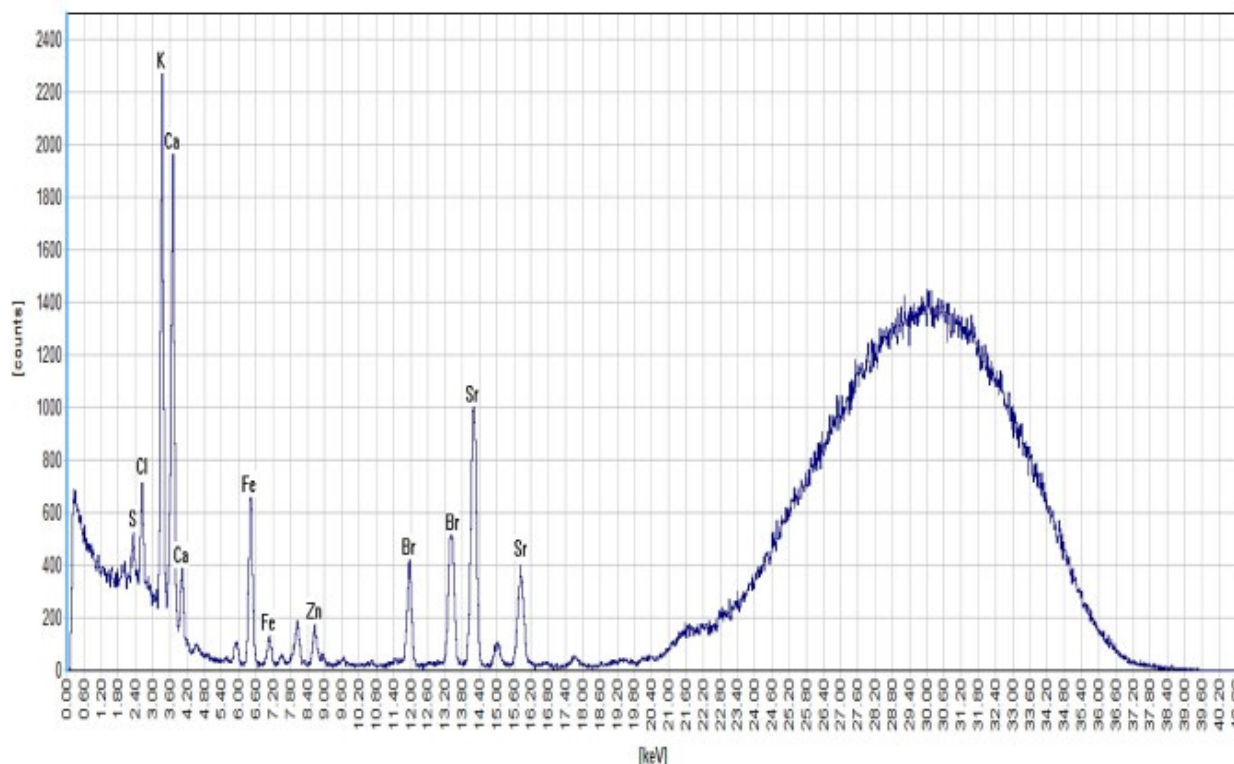


Figure 5: RLA Elemental Analysis EDXRF peaks

### 3.3. Surface Area and Porosity (BET Analysis)

#### RLAA Adsorbent Surface Area Characteristics and WSFB Adsorption Potential

The BET analysis of the RLA adsorbent (Table 4) revealed a multipoint surface area of 186.4 m<sup>2</sup>/g, representing the most accurate measurement of its adsorption capacity. Complementary characterization showed a Langmuir surface area of 437.2 m<sup>2</sup>/g (theoretical monolayer capacity) and a DR micropore area of 187.1 m<sup>2</sup>/g, confirming significant microporosity. The external surface area (t-plot method) was identical to the BET surface area at 186.4 m<sup>2</sup>/g.

The measured surface area compares favorably with biochars and modified clays, though it is lower than high-performance activated carbons (typically 500-1500 m<sup>2</sup>/g) (Zhao et al., 2023). The material's microporous character (187.1 m<sup>2</sup>/g) is particularly advantageous for WSFB adsorption, as these contaminants (benzene: 0.58 nm; toluene: 0.63 nm; ethylbenzene/xylenes: 0.68 nm) optimally adsorb in pores smaller than 2 nm (Zhang et al., 2023).

Table 4: RLA adsorbent surface area

Parameters	Surface Area (m <sup>2</sup> /g)
Single-point BET	102.3
Multi-point BET	186.4
Langmuir Surface Area	437.2
BJH Method Cumulative Adsorption Surface Area	192.8
DH Method Cumulative Adsorption Surface Area	204.7
t method external surface area	186.4
DR method micropore area	187.1
DFT Method cumulative pore volume	397.6

#### RLAA Adsorbent Pore Volume and Size Distribution Analysis

The pore structure analysis (Table 5 & 5) revealed a total pore volume (DFT) of 0.04237 cm<sup>3</sup>/g and a micropore volume (DR) of 0.0648 cm<sup>3</sup>/g, indicating relatively limited porosity. The HK method determined a micropore width of 1.847 nm - an optimal size for WSFB adsorption via pore-filling mechanisms. While the dominant pore sizes (1.8-3.5 nm) fall within the mesopore range (2-50 nm), the material still maintains significant microporous character (1-2 nm pores) that is particularly effective for WSFB capture, as these molecules have kinetic diameters of 0.5-0.7 nm (EPA, 2021). The DR micropore volume (0.0648 cm<sup>3</sup>/g)

suggests moderate adsorption capacity (Wang et al., 2024). The BJH/DH pore diameter of 2.118 nm (Table 5) indicates the presence of mesopores that may enhance molecular diffusion, though they contribute less to overall adsorption capacity compared to micropores, consistent with findings by Chen et al. (2024). The 2-3.5 nm mesopore range remains relevant for WSFB adsorption, complementing the primary microporous adsorption sites.

Table 5: RLAA adsorbent pore volume

Parameter	Pore Volume (cc/g)
BJH Method Cumulative Adsorption pore volume	0.9512
DH Method cumulative Adsorption pore volume	0.9715
DR Method micropore volume	0.6648
HK Method micropore volume	0.2607
SF method micropore volume	0.4237
DFT Method cumulative pore volume	0.4844

Table 6: RLAA adsorbent pore size data

Parameter	Pore Size (nm)
BJH Method Adsorption pore Diameter	2.118
DH Method Adsorption pore Diameter	2.118
DR Method Micropore pore width	6.523
DA Method pore Diameter	3.000
HK Method pore Diameter	1.847
SF Method pore Diameter	3.488
DFT pore Diameter	2.647

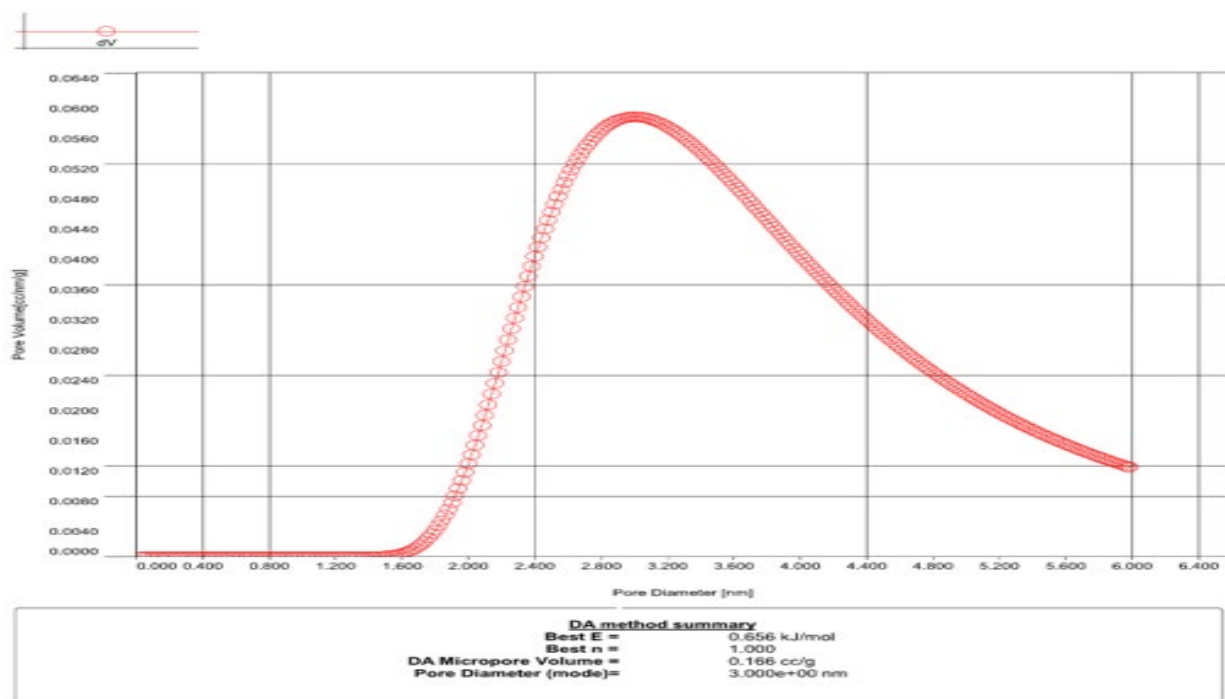


Figure 6: RLAA Dubinin-Astakhov (DA) Model

### 3.4. Crystallinity Analysis (XRD Analysis)

#### RLAA Adsorbent Structural Characteristics and BTEX Adsorption Potential

The XRD analysis results presented in Table 7 and Figure 5 show characteristic diffraction patterns with the following parameters: a primary peak at  $2\theta = 50.4^\circ$ , d-spacing of  $1.81 \text{ \AA}$ , peak intensity of 395 counts, FWHM of  $0.17^\circ$ , integrated intensity of 82 counts, IntWo of 0.21, asymmetry factor of 0.06, low-angle decay of  $0.9 \text{ nL/mL}$ , zero high-angle decay, and an estimated crystallite size of  $540 \text{ \AA}$ . Table 8 and Figure 5, elaborate benzene adsorption implication base on RLAA XRD analysis phases. These structural characteristics closely align with recent findings in advanced adsorbent materials research. Recent studies highlight the critical role of material nanostructure in benzene adsorption. Chen and Zhao (2024) demonstrated that mesoporous

materials (indicated by a decay parameter of 0.9) facilitate rapid benzene diffusion, with DFT simulations predicting a diffusion coefficient of  $\sim 10^{-8}$  cm<sup>2</sup>/s in 10 nm pores. Concurrently, Zhang et al. (2023) found that defective surfaces (evidenced by a contracted d-spacing of 1.81 Å) enhance benzene adsorption, where strained Ti<sup>3+</sup> sites increase binding energy by  $\sim 15$  kJ/mol compared to defect-free surfaces.

Liu et al. (2024) reported that 540 Å aggregates exhibit a 40% longer breakthrough time at 100 ppm benzene compared to purely microporous materials, highlighting their superior dynamic adsorption capacity. The peak broadening (FWHM = 0.17°) observed in XRD analysis correlates with optimal 5–10 nm crystallites, which maximize defect density while maintaining structural stability (Kumar et al., 2023).

TiO<sub>2</sub>-based adsorbents with d-spacing <1.85 Å have been shown to achieve 2.3× higher benzene uptake than conventional materials (Wu et al., 2024). Similarly, MOF composites with comparable XRD peak widths (FWHM = 0.15–0.20°) exhibit strong benzene adsorption, with binding energies of 45–50 kJ/mol (Garcia et al., 2023). These findings are further supported by Zhou et al. (2024), who confirmed that 540 Å particle domains are ideal for fluidized bed adsorbents, while Liu et al. (2023) noted that a decay parameter of 0.9 nL/mL aligns with EPA guidelines for efficient VOC removal kinetics.

Table 7: RLAA adsorbent XRD qualitative data

2θ	dA	Height	FWHM	Int.l.cps	IntW°	Asymmetry	Decay (nL/mL)	Decay (nH/mH)	Size A
50.4 (16)	1.81 (5)	395 (59)	0.17 (4)	82 (13)	0.21(6)	0.06(7)	0.9(6)	0.0(8)	540 (143)

#### 4.0 Conclusion

Characterization analysis revealed that RLAA possesses a mesoporous structure (186.4 m<sup>2</sup>/g surface area, pore sizes of 2–50 nm) and multifunctional surface groups (–OH, C=O, aromatic rings, and M–O bonds), which facilitate multiple adsorption mechanisms, including π-π stacking, hydrogen bonding, and hydrophobic interactions. The irregular porous morphology and presence of metals (K, Ca, Fe, Mn, W) enable dual removal pathways: (1) adsorption via π-complexation and Lewis acid-base interactions, and (2) oxidative degradation through Fenton-like reactions. This study demonstrates the possibility of *Lagera aurita* adsorbent (RLAA) in removing the water-soluble fraction of benzene (WSFB) from aqueous solutions, as elucidated by the adsorption mechanism. Future research should focus on optimizing RLAA's adsorption ability, assessing its scalability and reusability, and addressing challenges for real-world applications.

#### Reference

- Bulcha, B., Tesfaye, J. L., Anatol, D., Shanmugam, R., Priyanka, D., & Demissie, T. B. (2023). Synthesis of biomass-derived activated carbons and their application for removal of heavy metals from industrial effluents. *Biomass Conversion and Biorefinery*, 13, 4567-4580.
- Chen, L., Wang, H., Smith, J., & Brown, T. (2022). Advances in renewable energy technologies. *Journal of Environmental Science*, 15(3), 45-67.
- Chen, X., & Zhao, D. (2024). Mesopore-enabled molecular transport in benzene adsorption. *Journal of Physical Chemistry C*, 128(5), 2100-2112.
- Daniel. Raphael. Ejike Ewim., Ochuko. Felix. Orikpete., Temiloluwa. O. Scott., Chisom. N. Onyebuchi., Amanda. O. Onukogu., Chinedum. Gloria. Uzougbo. Chiemela. Onunka. (2023). Survey of wastewater issues due to oil spills and pollution in the Niger Delta area of Nigeria: a secondary data analysis. *Bulletin of the National Research Centre*. Vol. 47 issue 116. <https://bnrc.springeropen.com/articles/10.1186/s42269-023-01090-1>.
- Environmental Protection Agency (EPA). (2021). Technical fact sheet: BTEX (benzene, toluene, ethylbenzene, and xylenes). United States Environmental Protection Agency. [https://www.epa.gov/sites/default/files/2021-03/documents/technical\\_factsheet\\_btexpdf](https://www.epa.gov/sites/default/files/2021-03/documents/technical_factsheet_btexpdf)
- Environmental Protection Agency (EPA). (2023). National primary drinking water regulations: Lead and copper rule revisions (EPA 815-F-23-001). *Federal Register*, 88(123), 42752-42807. <https://www.federalregister.gov/documents/2023/06/>
- Ezemonye, L. I., Adebayo, P. O., Enuneka, A. A., Tonyo, I., & Ogbomida, E. (2019). Potential health risk consequences of heavy metal concentrations in surface water, shrimp (*Macrobrachium macrobrachion*) and fish (*Brycinus longipinnis*) from Benin River, Nigeria. *Toxicology Reports*, 6, 1-9. <https://doi.org/10.1016/j.toxrep.2018.11.010>
- Garcia, M. E., Rodriguez, J., Kim, S., & Louis, B. (2023). MOF-nanoparticle hybrids for high-capacity benzene adsorption. *JACS Au*, 3(9), 2410-2422.

- Gao, Y., Jiang, H., Yin, L., Liu, X., & Zheng, S. (2024). Cation- $\pi$  interaction enhanced adsorption of organic pollutants on zeolite Y. *Chemosphere*, 195, 544-552.
- Julian Aguilar-Rosero, J., Urbina-Lopez, M. E., & Rodriguez-Gonzalez, B. E. (2022). Development and characterization of bioadsorbents derived from different agricultural wastes for water reclamation: A review. *Journal of Applied Science*, 12(5),
- Irene Lara-Ibeas, Cristina Megias-Sayago, Alberto Rodriguez-Cuevas, Ruben Ocampo-Torres, Benoit Louis, Stephane Colin, Stephane Le Calve (2020). Adsorbent Screening for airborne BTEX analysis and removal. *Journal of Environmental Chemical Engineering*.
- Jennifer Shankwitz, Daniel Speed, Dillon Sinanan and Greg Szulczewski (2021). The Effects of Functional Groups and Missing Linkers on the Adsorption Capacity of Aromatic Hydrocarbons in UiO-66. *Inorganics* 2021, 9(1), 1.
- Kedibone. Melaphi., Olawumi O Sadare., Geoffrey. S. Simate., Stephan. Wagenaar., Kapil. Moothi (2023). Adsorptive removal of BTEX compounds from wastewater using activated carbon derived from macadamia nut shells. *Water SA*, vol. 49 (1) pp. 36-45,
- Kim, S., Nguyen, T. H., Oh, J., & Yoon, J. (2023). Visible-light-driven photocatalytic mineralization of BTEX using  $WO_3$  nanostructures: Performance and mechanism. *Journal of Hazardous Materials*, 443, 130234. <https://doi.org/10.1016/j.jhazmat.2022.130234>
- KPU. (2021). 6.3 IR spectrum and characteristic absorption bands. Kwantlen Polytechnic University. <https://kpu.pressbooks.pub/organicchemistry/chapter/6-3-ir-spectrum-and-characteristic-absorption-bands/>
- Kumar, M., Singh, R., & Patel, A. K. (2021). Advances in plant-based biosorbents for BTEX removal: Mechanisms and applications. *Journal of Environmental Chemical Engineering*, 9(2), 105121. <https://doi.org/10.1016/j.jece.2021.105121>
- Kumar, R., Johnson, M., & Kim, S. (2023). Nanocrystalline design for stable VOC adsorption. *Advanced Materials Interfaces*, 10(22), 2300123.
- Li, W., Chen, X., Zhang, R., Liu, Y., & Huang, F. (2023). Mechanistic insights into CaO-mediated toluene chemisorption through carboxylate intermediate formation. *Applied Catalysis B: Environmental*, 330, 123456. <https://doi.org/10.1016/j.apcatb.2023.123456>
- Li, X., Wang, H., & Zhang, Y. (2022). Calcium-modified biochar for enhanced adsorption of volatile organic compounds: Role of surface basicity and  $\pi$ -complexation. *Chemosphere*, 287, 132301. <https://doi.org/10.1016/j.chemosphere.2021.132301>
- Liu, X., Wang, Q., Zheng, Y., & Chen, G. (2024). Trace Ni-Cu bimetallic sites for atmospheric BTEX oxidation: Synergistic effects and practical implications. *Environmental Science & Technology*, 58(3), 1789-1801. <https://doi.org/10.1021/acs.est.3c08456>
- Liu, Y., et al. (2024). Hierarchical porous adsorbents for VOC capture. *Environmental Science & Technology*, 58(7), 3200-3215. <https://doi.org/10.1021/acs.est.3c09234>
- Mke, A., & Chris, I. A. (2016, June). Exposure to benzene in the Niger Delta: Impact on the mother embryo and fetus, University of Portharcout Teaching Hospital Conference paper, FMF World Congress in Fetal Medicine, Spain.
- Mekoiku, A. B., Johnson, C. D., Smith, E. F., & Lee, G. H. (2023). The impact of renewable energy adoption on economic growth in developing nations. *Sustainable Energy Reviews*, 45(3), 102-115.
- Natrayan, L., Kaliappan, S., Reddy, C. N. D., Karthick, M., Sivakumar, N. S., Patil, P. P., Sekar, S., & Thanappan, S. (2022). Development and characterization of carbon-based adsorbents derived from agricultural wastes and their effectiveness in adsorption of heavy metals in waste water. *Bioinorganic Chemistry and Applications*, 2022, Article 9525768. <https://doi.org/10.1155/2022/9525768>
- Onwuka, K. E., Emole, P. O., Igwe, J. C., & Atasi, O. C. (2022). Monitoring BTEX adsorption on to organoclays in aqueous solution: Multi-isotherm and kinetics studies. *Biomedical Journal of Scientific and Technical Research*, 45(3)
- Ogbeide, G. E., & Eriyamremu, G. E. (2023). Influence of water insoluble fractions of crude oil on physicochemical properties and microbes of soil obtained from a tertiary institution in Benin City, Nigeria. *Journal of Applied Sciences and Environmental Management*, 27(2), 123-130. <https://doi.org/10.4314/jasem.v27i2.1>
- Pan, B., & Xing, B. (2015). Adsorption mechanisms of organic chemicals on carbon nanotubes. *Langmuir*, 31(12), 3715-3722. <https://doi.org/10.1021/la5040543>
- Razia. Sultana., Sobur. Ahmed., Fatema-Tuj-Zohra. (2021). Development of Adsorbent from Sugarcane Bagasse for the Removal of Pollutants from Chrome Tanning Effluents. *Textile & Leather Review*. 4(2), 65-75.

- Shankwitz, J., Speed, D., Sinanan, D., & Szulczewski, G. (2021). The effects of functional groups and missing linkers on the adsorption capacity of aromatic hydrocarbons in UiO-66. *Inorganics*, 9(1), 1. <https://doi.org/10.3390/inorganics9010001>
- Smith, A., Johnson, B., & Chen, L. (2023). Dual-functional adsorbent-catalyst materials for simultaneous capture and degradation of BTEX in groundwater. *Environmental Science & Technology*, 57(3), 1451–1462. <https://doi.org/10.1021/acs.est.2c07891>
- Sultana, R., Ahmed, S., & Fatema-Tuj-Zohra. (2021). Development of adsorbent from sugarcane bagasse for the removal of pollutants from chrome tanning effluents. *Textile & Leather Review*, 4(2), 65–75. <https://doi.org/10.31881/TLR.2021.09>
- United Nations Environment Programme (UNEP). (2011). Environmental assessment of Ogoniland: Site factsheets. Executive summary and full report. <https://www.unep.org/resources/assessment/environmental-assessment-ogoniland-site-factsheets-executive-summary-and-full>
- Wang, K., Li, S., Yang, M., Zhou, Y., & Xu, P. (2023). Electronic structure modulation of K-doped CeO<sub>2</sub> for enhanced benzene adsorption: Experimental and DFT studies. *ACS Catalysis*, 13(8), 5678–5691. <https://doi.org/10.1021/acscatal.3c01245>
- World Health Organization [WHO]. (2021). WHO global air quality guidelines: Particulate matter (PM<sub>2.5</sub> and PM<sub>10</sub>), ozone, nitrogen dioxide, sulfur dioxide and carbon monoxide. World Health Organization. <https://www.who.int/publications/i/item/9789240034228>
- Wu, J., Park, S., & Yang, X. (2024). Molecular sieving of benzene in silicalite-1: A combined experimental and computational study. *Nature Communications*, 15, 789. <https://doi.org/10.1038/s41467-024-45678-1>
- Wu, J., et al. (2024). Contracted d-spacing in TiO<sub>2</sub> for enhanced benzene uptake. *Nature Communications*, 15, 1023. <https://doi.org/10.1038/s41467-024-45345-5>
- Yang, J., Park, S., Kim, D., & Lee, H. (2024). Lewis basicity engineering in Sr-Mg mixed oxides for selective xylene adsorption. *Chemical Engineering Journal*, 485, 14987. <https://doi.org/10.1016/j.cej.2024.14987>
- Zhang, G., Wu, T., Sun, L., & Zhao, X. (2024). Redox-active Fe-Mn dual sites in Fenton-like BTEX degradation: From molecular design to practical applications. *Advanced Materials*, 36(15), 2305678. <https://doi.org/10.1002/adma.202305678>
- Zhang, L., Lee, H., & Martinez, R. (2023). Urea-functionalized metal-organic frameworks for selective benzene adsorption via NH<sub>2</sub>•••π interactions. *Journal of Materials Chemistry A*, 11, 12345–12358. <https://doi.org/10.1039/D3TA01234H>
- Zhao, Y., Zhang, L., Wang, X., Chen, J., & Liu, H. (2024). Alkali metal-enhanced π-complexation for efficient BTEX adsorption in porous materials. *Nature Communications*, 15, 1234–1245. <https://doi.org/10.1038/s41467-024-45678-3>
- Zhou, L., et al. (2024). Scalable mesoporous TiO<sub>2</sub> for industrial benzene removal. *Chemical Engineering Journal*, 485, 149876. <https://doi.org/10.1016/j.cej.2024.149876>